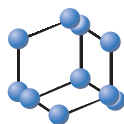


RESEARCH ARTICLE

BENTHAM
SCIENCE

Design and Synthesis of the Diazirine-based Clickable Photo-Affinity Probe Targeting Sphingomyelin Synthase 2



Penghui Wang, Zhining Li, Lulu Jiang, Lu Zhou* and Deyong Ye*

Department of Medicinal Chemistry, School of Pharmacy, Fudan University, Shanghai, P. R. China

Abstract: Background: SMS family plays a very important role in sphingolipids metabolism and is involved in the membrane mobility and signaling transduction.

Methods: SMS2 subtype was related to a variety of diseases and could be regarded as a promising potential drug target. However, the uncertainty of the binding sites and the molecular mechanism of action limited the development of SMS2 inhibitors. Herein, we discovered a photo-affinity probe **PAL-1** targeting SMS2.

Results: The enzyme inhibitory activity and the photo-affinity labeling experiments showed that **PAL-1** could be mono-labeled on SMS2.

Conclusion: In summary, starting from the *N*-arylbenzamides core structure and the minimalist terminal alkyne-containing diazirine photo-crosslinker, we designed and synthesized a photo-affinity probe **PAL-1** targeting SMS2. The enzymatic inhibitory activity study showed that **PAL-1** exhibited superior selectivities for SMS2 with an IC₅₀ of 0.37 μM over SMS1.

ARTICLE HISTORY

Received: March 18, 2018
Revised: October 19, 2018
Accepted: November 01, 2018

DOI:
10.2174/1570180816666181106154601



Keywords: Sphingomyelin synthase 2, sphingomyelin, photo-affinity labeling, diazirine, phosphatidylcholine, phosphoethanolamine.

1. INTRODUCTION

Sphingomyelin synthase (SMS) is the last step enzyme in the *de novo* synthesis of sphingomyelin in mammals, catalyzing the conversion of phosphatidylcholine (PC) and ceramide to diacylglycerol (DAG) and sphingomyelin (SM). SMS has three isoforms with different subcellular localizations. Sphingomyelin synthase 1 (SMS1) mainly localized in Golgi membrane, was believed to undertake the majority of SM production in the cell. Whereas, sphingomyelin synthase 2 (SMS2) is predominantly localized in the plasma membrane, although a minority portion was found in Golgi. Sphingomyelin synthase related protein (SMSr) with the weak function of ceramide phosphoethanolamine (CPE) production rather than the function of SM production, is mainly localized in the endoplasmic reticulum. These three SMSs regulate the levels of sphingomyelin and other sphingolipids to regulate the membrane mobility, as well as signaling transduction [1-3].

Recently, more and more investigations showed that the overexpression or dysfunction of SMSs was related to a variety of diseases [3]. SMS1 was found to be necessary for insulin secretion and mitochondrial function [4]. SMS1 deficiency may cause hearing impairments [5], male infertility [6] and other serious metabolic abnormalities in mice [4]. Interestingly, SMS2 overexpression was involved in

inflammation [7] and metabolic disorders such as atherosclerosis [8, 9], diabetes [10], and obesity [11]. SMS2 deficiency could attenuate LPS-induced lung injury [12], decrease atherosclerosis in mice [13], and impair insulin sensitivity [14] and secretion [15] in mice. Besides, SMS2 was also involved in the HIV-1 infection [16] and the induction of murine colitis-associated colon cancer [17]. These studies suggested that SMS2 could be regarded as a promising drug target for the diseases mentioned above to drive the discovery of SMS2 inhibitors (Fig. 1) [18-20].

All the three isoforms of SMS share high sequence identity with each other and are predicted as six-pass transmembrane proteins, which brought challenges to understand the molecular mechanism of actions and characterize the structure of SMSs through crystallography [21]. Although the 3D structure model of SMS1 has been generated by homology modeling, the validity of this constructed model is not experimentally demonstrated and exposed to the risk of over-interpretation due to the low sequence similarities between the homologous protein and the template proteins [22]. The interaction between SMSs and their small molecular inhibitors still remains unclear that limits the further development of SMS2 inhibitors as so far.

Photo-affinity labeling (PAL) is an effective strategy in structural biology that uses a chemical probe to generate photoactive intermediate under the irradiation of the light with a specific wavelength for subsequent covalently binding to its target. Cooperating with the activity-based protein profiling (ABPP) and the mass spectrometry, PAL has been widely used in chemical biology and drug discovery for target identification, molecular interactions confirmation and

*Address correspondence to these authors at the Department of Medicinal Chemistry, School of Pharmacy, Fudan University, Shanghai, P. R. China; Tel/Fax: +86-21-51980125 (Lu Zhou), +86-21-51980117 (Deyong Ye); E-mails: zhoulu@fudan.edu.cn (Lu Zhou); dyye@shmu.edu.cn (Deyong Ye)

for probing the location and structure of binding sites [23-29]. Herein, we adopted the PAL strategy to design and synthesize the photo-affinity probe targeting sphingomyelin synthase 2, thus providing a chemical tool for exploring the binding sites and the interaction of small molecules with SMS2.

2. EXPERIMENTAL SECTION

2.1. The Procedures of PAL-1's Preparation

2.1.1. 2-(3-(But-3-yn-1-yl)-3H-diazirin-3-yl)ethan-1-ol (2)

Compound **1** (173 mg, 1.37 mmol) was dissolved in anhydrous ammonia (10 mL). After stirring for 2 h at -78°C , a solution of hydroxylamine-*O*-sulfonic acid (187 mg, 1.65 mmol) in 1 mL dry methanol was added dropwise. The reaction system was allowed to stirring overnight. The resulting slurry was diluted with ethyl acetate (5 mL) and filtered. The filtrate was concentrated under reduced pressure and the residue was re-dissolved in dry dichloromethane (10 mL) and treated with triethylamine (0.83 mL, 5.94 mmol) subsequently. A solution of iodine (665 mg, 2.62 mmol) in dichloromethane (10 mL) was slowly added with stirring until the reaction solution was turned into orange-brown. The reaction mixture was continuously stirring for another 2 h and a solution of sodium thiosulfate (1 mol/L, 10 mL) in water was added. The organic phase was washed with brine, dried over sodium sulfate and concentrated under reduced pressure. The residue was purified by flash column chromatography to give a colorless oil (60 mg, yield: 32%). ^1H NMR (400 MHz, Chloroform-*d*) δ 3.50 (q, $J = 5.7$ Hz, 2H), 2.05 (td, $J = 7.4, 2.5$ Hz, 2H), 2.01 (t, $J = 2.4$ Hz, 1H), 1.71 (dt, $J = 11.3, 6.7$ Hz, 4H), 1.48 (t, $J = 4.5$ Hz, 1H). ^{13}C NMR (151 MHz, CDCl_3) δ 82.85, 69.23, 57.42, 35.56, 35.52, 32.68, 26.60, 13.25.

2.1.2. 3-(2-Bromoethyl)-3-(but-3-yn-1-yl)-3H-diazirine (3)

To a solution of compound **2** (172 mg, 1.24 mmol) in dry dichloromethane (5 mL), CBr_4 (620 mg, 1.87 mmol) and PPh_3 (450 mg, 1.87 mmol) were added at r.t. After stirring for 4 h, the reaction mixture was concentrated under reduced pressure. The residue was dissolved in ethyl ether and filtered to remove the insoluble triphenylphosphine oxide. The filtrate was concentrated under reduced pressure and the residue was purified by flash column chromatography to give a colorless oil (160 mg, 64%). ^1H NMR (400 MHz, Chloroform-*d*) δ 3.17 (t, $J = 7.2$ Hz, 2H), 2.09 – 1.97 (m, 5H), 1.71 (t, $J = 7.3$ Hz, 2H). ^{13}C NMR (151 MHz, CDCl_3) δ 82.45, 69.42, 36.46, 32.05, 27.41, 25.59, 13.25.

2.1.3. (2-(2-(3-(But-3-yn-1-yl)-3H-diazirin-3-yl)ethoxy)phenyl)methanol (4)

Compound **3** (160 mg, 0.796 mmol), salicyl alcohol (120 mg, 0.955 mmol) and potassium carbonate (165 mg, 1.19 mmol) were added into acetonitrile (10 mL) and heated to 80°C for 4 h. After cooling to r.t, the reaction mixture was diluted with ethyl acetate (5 mL) and filtered to remove the potassium carbonate. The filtrate was concentrated under reduced pressure and the residue was purified by flash column chromatography to give a colorless oil (120 mg,

62%). ^1H NMR (400 MHz, Chloroform-*d*) δ 7.32 – 7.22 (m, 2H), 6.96 (t, $J = 7.5$ Hz, 1H), 6.80 (d, $J = 8.2$ Hz, 1H), 4.74 (s, 2H), 3.85 (t, $J = 5.9$ Hz, 2H), 2.13 – 1.97 (m, 5H), 1.74 (t, $J = 7.4$ Hz, 2H). ^{13}C NMR (151 MHz, CDCl_3) δ 156.20, 129.37, 129.23, 128.98, 121.09, 110.76, 82.59, 69.43, 62.33, 61.97, 32.53, 32.38, 26.85, 13.26.

2.1.4. 2-((2-(2-(3-(But-3-yn-1-yl)-3H-diazirin-3-yl)ethoxy)benzyl)-oxy)-*N*-(pyridin-3-yl)benzamide hydrochloride (PAL-1·HCl)

To a solution of compound **4** (90 mg, 0.368 mmol) in dry tetrahydrofuran (20 mL), PPh_3 (145 mg, 0.553 mmol) and 2-hydroxy-*N*-(pyridin-3-yl)benzamide (80 mg, 0.368 mmol) were added. After stirring for 5 min at 0°C , DEAD (90 μL , 0.553 mmol) was injected into the reaction mixture through a syringe under a nitrogen atmosphere. The reaction was completed after another 2 h monitored by TLC. The mixture was diluted with ethyl acetate (10 mL) and saturated NH_4Cl solution (15 mL). The organic phase was washed with brine, dried over sodium sulfate and concentrated under reduced pressure. The residue was purified by flash column chromatography to give a crude product (120 mg) containing triphenylphosphine oxide.

The above crude product was dissolved in ethyl acetate (2 mL). Hydrogen chloride in ethyl acetate (1 mol/L, 1 mL) was added dropwise under vigorous stirring. The reaction solution gradually became cloudy. After stirring for 1 h, the mixture was filtered and the filter cake was recrystallized in $\text{Et}_2\text{O}/\text{EtOAc}$ three times to give a white solid PAL-1 hydrochloride (13 mg, yield:12%). ^1H NMR (400 MHz, DMSO-*d*₆) δ 10.84 (s, 1H), 9.06 (s, 1H), 8.54 (d, $J = 5.6$ Hz, 1H), 8.31 (s, 1H), 7.81 (s, 1H), 7.72 (d, $J = 7.2$ Hz, 1H), 7.58 (t, $J = 8.0$ Hz, 1H), 7.48 (d, $J = 8.2$ Hz, 1H), 7.31 (t, $J = 7.8$ Hz, 2H), 7.14 (t, $J = 7.5$ Hz, 1H), 7.02 (d, $J = 8.2$ Hz, 1H), 6.92 (t, $J = 7.4$ Hz, 1H), 5.33 (s, 2H), 3.86 (t, $J = 6.0$ Hz, 2H), 2.82 (t, $J = 2.8$ Hz, 1H), 1.96 (td, $J = 7.6, 2.8$ Hz, 2H), 1.84 (t, $J = 5.9$ Hz, 2H), 1.60 (t, $J = 7.4$ Hz, 2H). ^{13}C NMR (151 MHz, DMSO) δ 165.07, 155.85, 155.49, 139.69, 137.05, 135.39, 132.82, 131.04, 129.87, 129.37, 128.63, 125.83, 124.18, 123.71, 120.85, 120.52, 113.31, 111.61, 82.94, 71.57, 65.54, 62.69, 31.67, 31.49, 26.85, 12.45. MS (ESI⁺) m/z 441.2 (M + H)⁺. HRMS (ESI⁺) m/z : 441.1922 (M + H)⁺ (calcd for Chemical Formula: $\text{C}_{26}\text{H}_{25}\text{N}_4\text{O}_3$ ⁺: 441.1921).

2.2. In Vitro SMS Enzyme Activity Assay

2.2.1. SMS1 Inhibitory Activities

5 μL PAL-1·HCl in DMSO with different concentrations was added to 75 μL SMS1 protein solution (0.041 $\mu\text{g}/\mu\text{L}$) in DDM buffer (containing 1mM DDM, 150 mM NaCl, and 20 mM Hepes, pH 7.5) and the mixture was incubated at room temperature for 5 min. Then, another 20 μL of DDM solution (containing 1 μL anhydrous ethanol solution of DMPC (40 mM) and 1 μL DMSO solution of C6-NBD-ceramide (1.16 mM)) were added. To the mixture, the sample was added, incubated at 37°C for 30 min and quenched with 200 μL anhydrous ethanol. After centrifuged at 10000 rpm for 10 min, the supernatant was collected for HPLC test.

2.2.2. SMS2 Inhibitory Activities

The assay was similar to that of SMS1 using 79 μL of the SMS2 protein solution (0.0041 $\mu\text{g}/\mu\text{L}$) in DDM and 1 μL of a DMSO solution of the compound instead of the above.

2.3. PAL-1 Photolysis Assay

A solution of PAL-1·HCl (100 μM) in methanol was irradiated by UV lamp (365nm, 40 W) on ice for 0 min, 10 min, 20 min, 40 min and 80 min, respectively. The samples were kept within 1 cm from the lamp. After irradiation, the samples were injected into the LC-MS system to measure the concentration ratios and molecular weight of PAL-1 and its photolysis product.

2.4. Photo-Affinity Labeling Experiment

To a solution of SMS2 in DDM (with the protein content of 1.6 $\mu\text{g}/\mu\text{L}$, 30 μL) 0.5 μL PAL-1·HCl was added in DMSO (4 mM). The solution was incubated for 30 min and subsequently irradiated by UV lamp (365nm, 40 W) on ice for 40 min. The samples were kept within 1 cm from the lamp. After irradiation, the samples were injected into the Agilent 6550 iFunnel Q-TOF LC/MS system to measure the molecular weight of the complex of PAL-1 labeled SMS2.

3. RESULTS AND DISCUSSION

As shown in Fig. 1, the inhibitors of SMS2 could be classified into four structural categories. The α -aminophenyl

acetonitriles were discovered as pan SMS inhibitors with low selectivity through virtual screening and molecular docking by using the homology modeling structure of SMS1 [18]. Starting optimization from the α -aminophenylacetonitriles, a series of oxazolopyridines [19] and *N*-arylbenzamides (our unpublished results) was obtained with improved activity and selectivity. The 2-quinolone derivatives were discovered through a high-throughput mass spectrometry-based screening system [20]. Considering the preliminary structure and activity relationship (SAR) of the *N*-arylbenzamides compounds (our unpublished data), we selected the *N*-arylbenzamide as the core of photo-affinity probe and installed the minimalist terminal alkyne-containing diazirine as the photo-crosslinker [30] to constitute the clickable photo-affinity probe PAL-1 (Fig. 2).

The PAL-1 was synthesized according to Scheme 1. The diazirine alcohol **2** was prepared as described in Li's work [30] and was transformed to the corresponding bromide **3** via Appel reaction. The bromide **3** was nucleophilically substituted by the salicylic alcohol to yield the substituted benzyl alcohol **4**. And then the alcohol **4** was condensed with the 2-hydroxy-*N*-(pyridin-3-yl)benzamide to afford the target molecule PAL-1 via Mitsunobu reaction, which was subsequently converted into the corresponding hydrochloride salt.

The inhibitory activities of the probe PAL-1 against the SMS1 and SMS2 were evaluated through the HPLC based assay [31] by using pure SMS1 and SMS2 proteins as

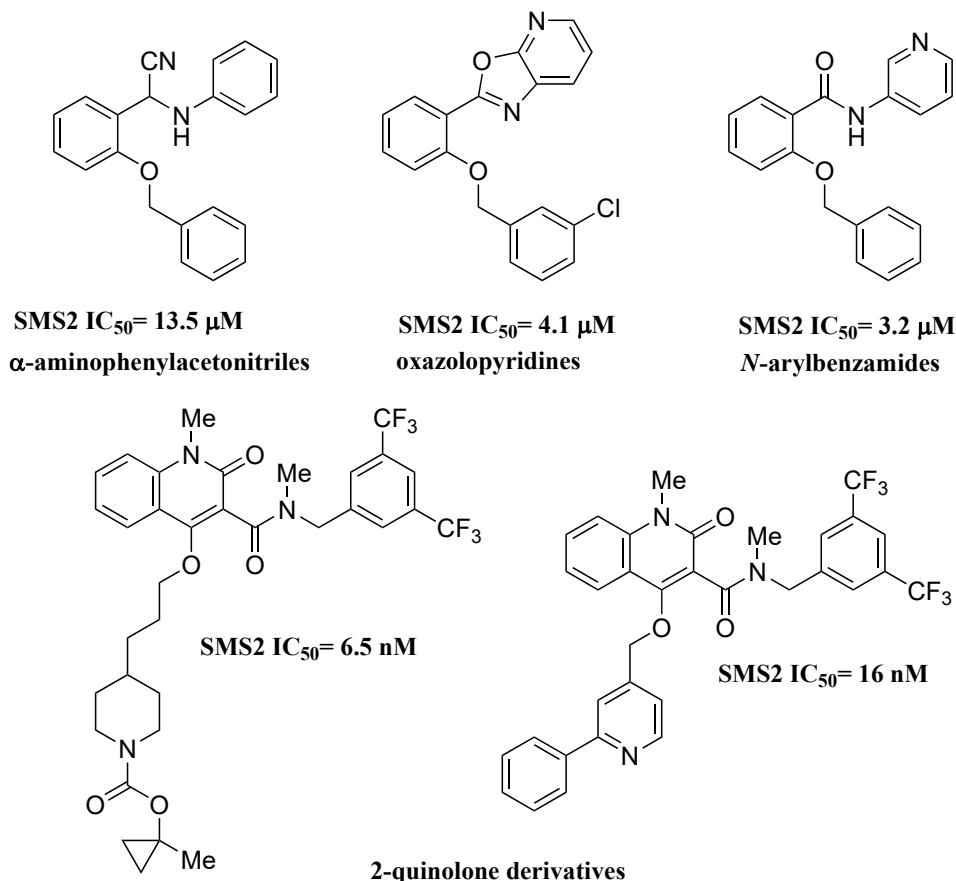


Fig. (1). The structures of representative SMS2 inhibitors.

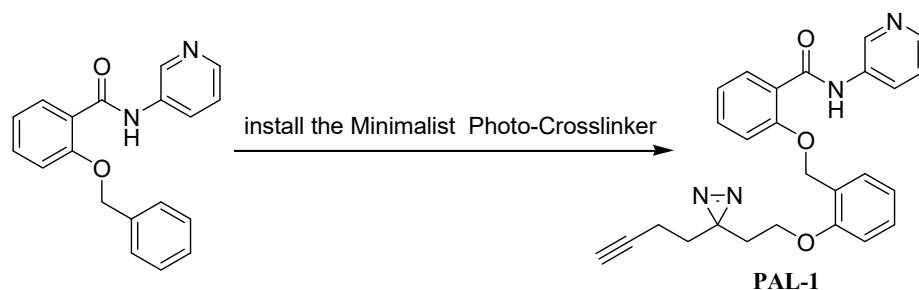
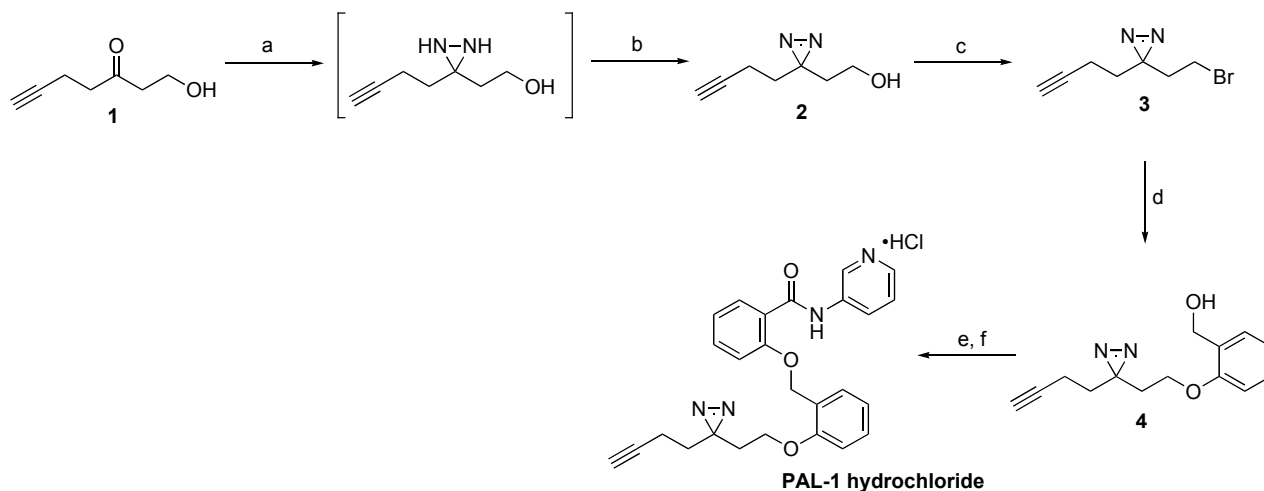


Fig. (2). The design of the photo -affinity probe.



Scheme 1. Reagents and conditions: **a.** NH_3 (l), then $\text{NH}_2\text{OSO}_3\text{H}$ in methanol, NH_3 (l), -78°C ; **b.** I_2 , NEt_3 , MeOH , r.t., 32% (2 steps); **c.** CBr_4 , PPh_3 , DCM , r.t., 64%; **d.** 2-(hydroxymethyl)phenol, K_2CO_3 , DMF , 80°C , 62%; **e.** 2-hydroxy-*N*-(pyridin-3-yl)benzamide, DEAD , PPh_3 , THF , 0°C ; **f.** HCl (1 mol/L) in EtOAc , Et_2O , r.t., 12% (2 steps).

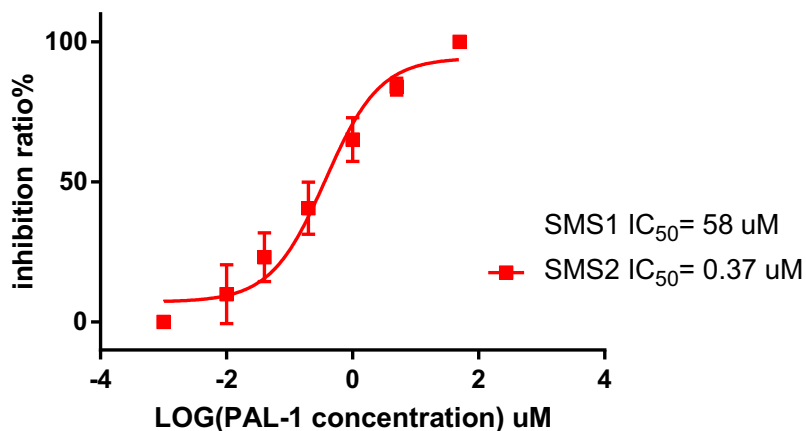


Fig. (3). The IC_{50} curves of PAL-1 against SMS1 and SMS2.

enzyme sources. As shown in Fig. 3, PAL-1 with an IC_{50} of 58 μM and 0.37 μM against SMS1 and SMS2 respectively showed 150-fold selectivity on SMS2 compared to on SMS1. The hydrophobic cross-linker on the C2 of benzyl group of the *N*-arylbenzamide could enhance the inhibitory activity, which was consistent with our previous work [19].

Prior to the labeling experiments with SMS2, the photochemical reactivity of PAL-1 in methanol was examined. The concentration ratio of PAL-1 with its

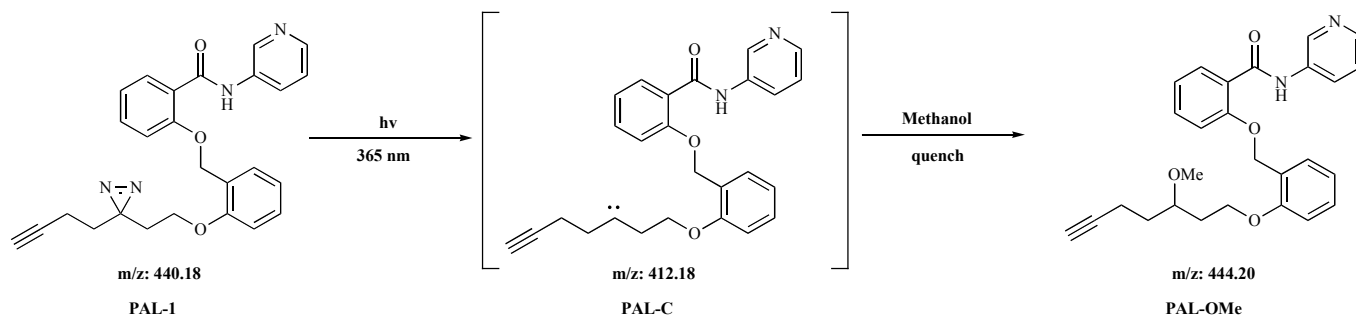
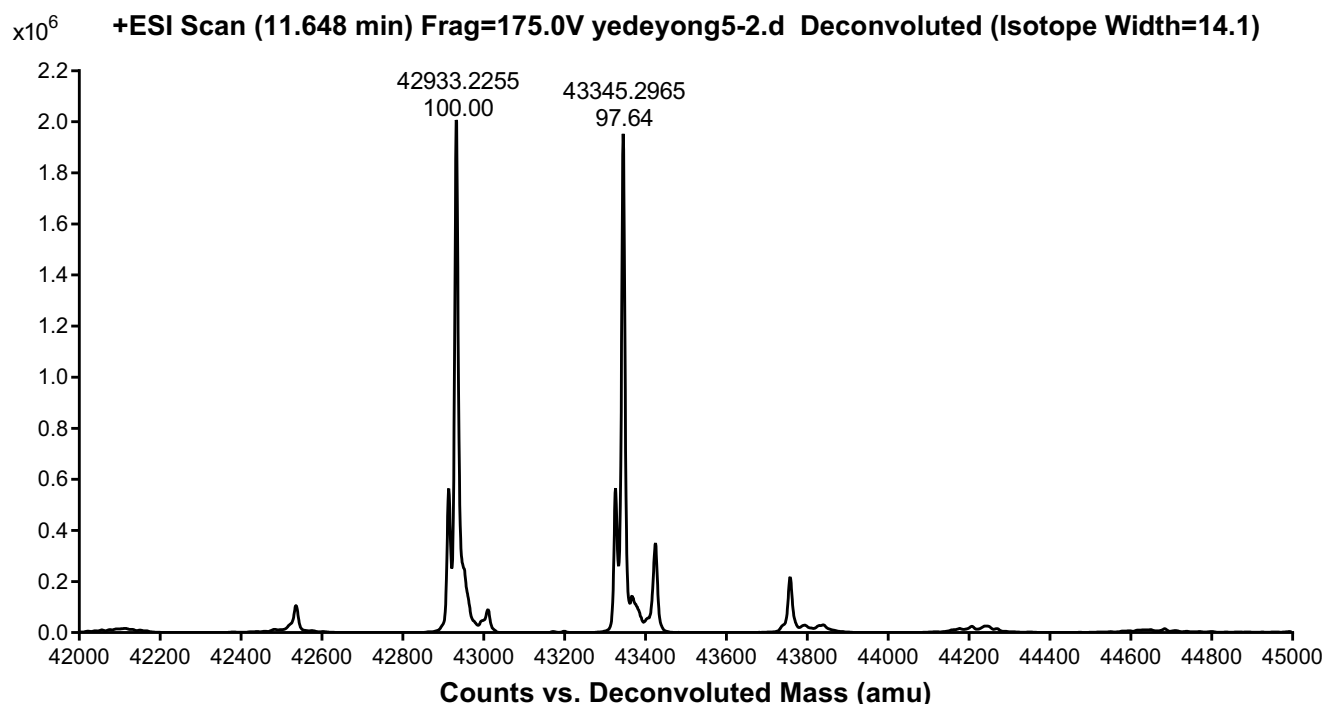
photolysis product was analyzed by LC-MS. As shown in Table 1, the concentration of the photolysis product was significantly increased in a time-dependent manner in the first 20 minutes. However, the photolysis efficiency was attenuated with the increase of time (40 and 80 minutes). In addition, the PAL-1 should be activated by UV light irradiation (365 nm) to generate the carbene intermediate PAL-C, which was then quenched by the solvent methanol to yield the intended methoxy product (Fig. 4) [32, 33]. To our surprise, the mass spectrum data revealed that the

Table 1. The concentration ratio of PAL-1 and its photolysis product analyzed by LC-MS.

Time(min)*	Concentration Ratio
0	100:0
10	73:27
20	32:68
40	22:78
80	20:80

*The PAL-1 in methanol (100 μ M) was irradiated with the UV light (365 nm) for different time.

photolysis product's m/z value was 412.2 rather than 444.2 in our system. We conjectured that the carbene intermediate PAL-C has undergone self-quenching before being quenched by solvent methanol.

**Fig. (4).** The intended photochemical reaction of PAL-1 in methanol.**Fig. (5).** The mass spectrum of photoaffinity labeling product of PAL-1 with SMS2.

After the above photochemical reactivity test, the labeling experiment was conducted on the pure SMS2 enzyme system. The PAL-1 was incubated with SMS2 for 30 minutes followed by UV light (365 nm) irradiation for 40 minutes. The sample was injected into the Agilent 6550 iFunnel Q-TOF LC/MS system to measure the molecular weight of the PAL-1 labeled SMS2. As shown in Fig. 5, the mass shift between the SMS2 (42933.2255) and the major PAL-SMS2 complex (43345.2965) was 412.0710, which was consistent with the molecular weight of the labeling fragment of PAL-1 after the loss of N_2 . This mass spectrum data proved that PAL-1 could mono-label the SMS2. As for the specific labeling sites, the further tryptic digestion for mass spectrometry analysis is still ongoing.

CONCLUSION

In summary, starting from the *N*-arylbenzamide core structure and the minimalist terminal alkyne-containing diazirine photo-crosslinker, we designed and synthesized a photo-affinity probe PAL-1 targeting SMS2. The enzymatic

inhibitory activity study showed that **PAL-1** exhibited superior selectivities for SMS2 with an IC₅₀ of 0.37 μM over SMS1. Besides, the **PAL-1**'s photolysis product in methanol was conjectured as the self-quenching product based on the molecular weight test. Moreover, the photoactivated labeling experiment of **PAL-1** with SMS2 was conducted and the labeled complex was identified as a mono-labeled product through the mass spectrum. Thus, we believed that **PAL-1** would be a chemical tool for probing the binding sites and the interaction of the small molecule inhibitors of SMS2. In addition, with this clickable photo-affinity probe **PAL-1**, the activity-based protein profiling (ABPP), the labeling site analysis, and the cell-based photo-affinity labeling are ongoing in our lab for further understanding the molecular mechanism of action of small molecules that bind to SMS2.

LIST OF ABBREVIATIONS

ABPP	=	Activity-Based Protein Profiling
CPE	=	Ceramide Phosphoethanolamine
PAL	=	Photo-Affinity Labeling
PC	=	Phosphatidylcholine
SM	=	Sphingomyelin
SMS	=	Sphingomyelin Synthase

CONSENT FOR PUBLICATION

Not applicable.

FUNDING

This study was financially supported by the Shanghai Municipal Committee of Science and Technology (No 17431902300), the program for Shanghai Rising Star (No 15QA1400300), and the Open Grant (2015-2017) of the State Key Laboratory of Bio-organic and Natural Products Chemistry, Chinese Academy of Sciences and the National Science & Technology Major Project "Key New Drug Creation and Manufacturing Program", China (No 2018ZX09711002).

CONFLICT OF INTEREST

The authors declare no conflict of interest, financial or otherwise.

ACKNOWLEDGEMENTS

Lu Zhou & Deyong Ye conceived and designed the research; Penghui Wang performed the experimental works and wrote the manuscript, Zhining Li and Lulu Jiang participated in the experimental works, analyzed the data and discussed the results. The authors also gratefully acknowledge Prof. Youhong Hu and Dr. Wenming Ren from the Shanghai Institute of Materia Medica, Chinese Academy of Sciences, and Dr. Chao Peng from the National Center for Protein Science (Shanghai) for providing the 365 nm UV lamp and the analysis of mass spectrometry of macromolecules respectively.

REFERENCES

- [1] Holthuis, J.; Ternes, P.; van den Dikkenberg, J.; Huitema, K. The sphingomyelin synthase family: Identification and biological implications. *Faseb. J.*, **2005**, *19*(5), A1371-A1371.
- [2] Tafesse, F.G.; Ternes, P.; Holthuis, J.C.M. The multigenic sphingomyelin synthase family. *J. Biol. Chem.*, **2006**, *281*(40), 29421-29425.
- [3] Chen, Y.; Cao, Y. The sphingomyelin synthase family: proteins, diseases, and inhibitors. *Biol. Chem.*, **2017**, *398*(12), 1319-1325.
- [4] Yano, M.; Watanabe, K.; Yamamoto, T.; Ikeda, K.; Senokuchi, T.; Lu, M.H.; Kadomatsu, T.; Tsukano, H.; Ikawa, M.; Okabe, M.; Yamaoka, S.; Okazaki, T.; Umehara, H.; Gotoh, T.; Song, W.J.; Node, K.; Taguchi, R.; Yamagata, K.; Oike, Y. Mitochondrial dysfunction and increased reactive oxygen species impair insulin secretion in sphingomyelin synthase 1-null mice. *J. Biol. Chem.*, **2011**, *286*(5), 3992-4002.
- [5] Lu, M.H.; Takemoto, M.; Watanabe, K.; Luo, H.; Nishimura, M.; Yano, M.; Tomimoto, H.; Okazaki, T.; Oike, Y.; Song, W.J. Deficiency of sphingomyelin synthase-1 but not sphingomyelin synthase-2 causes hearing impairments in mice. *J. Physiol.*, **2012**, *590*(16), 4029-4044.
- [6] Wittmann, A.; Grimm, M.O.W.; Scherthan, H.; Horsch, M.; Beckers, J.; Fuchs, H.; Gailus-Durner, V.; de Angelis, M.H.; Ford, S.J.; Burton, N.C.; Razansky, D.; Trumbach, D.; Aichler, M.; Walch, A.K.; Calzada-Wack, J.; Neff, F.; Wurst, W.; Hartmann, T.; Floss, T. Sphingomyelin synthase 1 is essential for male fertility in mice. *PLoS One*, **2016**, *11*(10), e0164298.
- [7] Zhao, Y.R.; Dong, J.B.; Li, Y.; Wu, M.P. Sphingomyelin synthase 2 over-expression induces expression of aortic inflammatory biomarkers and decreases circulating EPCs in ApoE KO mice. *Life Sci.*, **2012**, *90*(21-22), 867-873.
- [8] Liu, J.; Zhang, H.Q.; Li, Z.Q.; Hailemariam, T.K.; Chakraborty, M.; Jiang, K.L.; Qiu, D.; Bui, H.H.; Peake, D.A.; Kuo, M.S.; Wadgaonkar, R.; Cao, G.Q.; Jiang, X.C. Sphingomyelin synthase 2 is one of the determinants for plasma and liver sphingomyelin levels in mice. *Arterioscl. Throm. Vas.*, **2009**, *29*(6), 850-U189.
- [9] Wang, X.G.; Dong, J.B.; Zhao, Y.R.; Li, Y.; Wu, M.P. Adenovirus-mediated sphingomyelin synthase 2 increases atherosclerotic lesions in ApoE KO mice. *Lipids Health Dis.*, **2011**, *10*, 7.
- [10] Mitsutake, S.; Zama, K.; Yokota, H.; Yoshida, T.; Tanaka, M.; Mitsui, M.; Ikawa, M.; Okabe, M.; Tanaka, Y.; Yamashita, T.; Takemoto, H.; Okazaki, T.; Watanabe, K.; Igarashi, Y. Dynamic modification of sphingomyelin in lipid microdomains controls development of obesity, fatty liver, and type 2 diabetes. *J. Biol. Chem.*, **2011**, *286*(32), 28544-28555.
- [11] Mitsutake, S.; Yokota, H.; Zama, K.; Yoshida, T.; Yamashita, T.; Okazaki, T.; Watanabe, K.; Igarashi, Y. Sphingomyelin synthase 2 is responsible for obesity and lipid droplet formation in liver and is a novel regulator of membrane microdomain. *Chem. Phys. Lipids*, **2011**, *164*, S16-S16.
- [12] Gowda, S.; Yeang, C.; Wadgaonkar, S.; Anjum, F.; Grinkina, N.; Cutaia, M.; Jiang, X.C.; Wadgaonkar, R. Sphingomyelin synthase 2 (SMS2) deficiency attenuates LPS-induced lung injury. *Am. J. Physiol. Lung C.*, **2011**, *300*(3), L430-L440.
- [13] Liu, J.; Huan, C.M.; Chakraborty, M.; Zhang, H.Q.; Lu, D.; Kuo, M.S.; Cao, G.Q.; Jiang, X.C. Macrophage sphingomyelin synthase 2 deficiency decreases atherosclerosis in mice. *Circ. Res.*, **2009**, *105*(3), 295-U205.
- [14] Li, Z.; Zhang, H.; Liu, J.; Liang, C.P.; Li, Y.; Li, Y.; Teitelman, G.; Beyer, T.; Bui, H.H.; Peake, D.A.; Zhang, Y.; Sanders, P.E.; Kuo, M.S.; Park, T.S.; Cao, G.; Jiang, X.C. Reducing plasma membrane sphingomyelin increases insulin sensitivity. *Mol. Cell Biol.*, **2011**, *31*(20), 4205-4218.
- [15] Zhou, H.; Gong, Y.; Yang, P.; Ma, Y.; Fu, Z.; Zhou, Y.; Fu, J.; Zhu, X.; Yang, T. Sphingomyelin synthase 2 deficiency impairs insulin secretion in pancreatic beta cells. *Diabetologia*, **2017**, *60*, S221-S222.
- [16] Hayashi, Y.; Nemoto-Sasaki, Y.; Tanikawa, T.; Oka, S.; Tsuchiya, K.; Zama, K.; Mitsutake, S.; Sugiura, T.; Yamashita, A. Sphingomyelin synthase 2, but not sphingomyelin synthase 1, is involved in HIV-1 envelope-mediated membrane fusion. *J. Biol. Chem.*, **2014**, *289*(44), 30842-30856.
- [17] Ohnishi, T.; Hashizume, C.; Taniguchi, M.; Furumoto, H.; Han, J.; Gao, R.F.; Kinami, S.; Kosaka, T.; Okazaki, T. Sphingomyelin

- synthase 2 deficiency inhibits the induction of murine colitis-associated colon cancer. *Faseb. J.*, **2017**, *31*(9), 3816-3830.
- [18] Deng, X.; Lin, F.; Zhang, Y.; Li, Y.; Zhou, L.; Lou, B.; Li, Y.; Dong, J.; Ding, T.; Jiang, X.; Wang, R.; Ye, D. Identification of small molecule sphingomyelin synthase inhibitors. *Eur. J. Med. Chem.*, **2014**, *73*, 1-7.
- [19] Qi, X.Y.; Cao, Y.; Li, Y.L.; Mo, M.G.; Zhou, L.; Ye, D.Y. Discovery of the selective sphingomyelin synthase 2 inhibitors with the novel structure of oxazolopyridine. *Bioorg. Med. Chem. Lett.*, **2017**, *27*(15), 3511-3515.
- [20] Adachi, R.; Ogawa, K.; Matsumoto, S.; Satou, T.; Tanaka, Y.; Sakamoto, J.; Nakahata, T.; Okamoto, R.; Kamaura, M.; Kawamoto, T. Discovery and characterization of selective human sphingomyelin synthase 2 inhibitors. *Eur. J. Med. Chem.*, **2017**, *136*, 283-293.
- [21] Huitema, K.; van den Dikkenberg, J.; Brouwers, J.F.H.M.; Holthuis, J.C.M. Identification of a family of animal sphingomyelin synthases. *Embo. J.*, **2004**, *23*(1), 33-44.
- [22] Zhang, Y.; Lin, F.; Deng, X.D.; Wang, R.X.; Ye, D.Y. Molecular modeling of the three-dimensional structure of human sphingomyelin synthase. *Chinese J. Chem.*, **2011**, *29*(8), 1567-1575.
- [23] Hatanaka, Y.; Sadakane, Y. Photoaffinity labeling in drug discovery and developments: Chemical gateway for entering proteomic frontier. *Curr. Top. Med. Chem.*, **2002**, *2*(3), 271-88.
- [24] Vodovozova, E.L. Photoaffinity labeling and its application in structural biology. *Biochem. Moscow.*, **2007**, *72*(1), 1-20.
- [25] Sumranjit, J.; Chung, S.J. Recent advances in target characterization and identification by photoaffinity probes. *Molecules*, **2013**, *18*(9), 10425-10451.
- [26] Smith, E.; Collins, I. Photoaffinity labeling in target- and binding-site identification. *Future Med. Chem.*, **2015**, *7*(2), 159-183.
- [27] Lapinsky, D.J.; Johnson, D.S. Recent developments and applications of clickable photoprobes in medicinal chemistry and chemical biology. *Future Med. Chem.*, **2015**, *7*(16), 2143-2171.
- [28] Murale, D.P.; Hong, S.C.; Haque, M.M.; Lee, J.S. Photo-affinity labeling (PAL) in chemical proteomics: A handy tool to investigate protein-protein interactions (PPIs). *Proteome Sci.*, **2017**, *15*, 14.
- [29] Muranaka, H.; Momose, T.; Handa, C.; Ozawa, T. Photoaffinity labeling in drug discovery research. In *Photoaffinity Labeling for Structural Probing Within Protein*, Hatanaka, Y.; Hashimoto, M. Eds. Springer Japan: Tokyo, **2017**; pp 241-265.
- [30] Li, Z.Q.; Hao, P.L.; Li, L.; Tan, C.Y.J.; Cheng, X.M.; Chen, G.Y. J.; Sze, S.K.; Shen, H.M.; Yao, S.Q. Design and synthesis of minimalist terminal alkyne-containing diazirine photo-crosslinkers and their incorporation into kinase inhibitors for cell- and tissue-based proteome profiling. *Angew. Chem. Int. Ed.*, **2013**, *52*(33), 8551-8556.
- [31] Deng, X.D.; Sun, H.; Gao, X.; Gong, H.J.; Lu, W.B.; Chu, Y.; Zhou, L.; Ye, D.Y. Development, validation, and application of a novel method for mammalian sphingomyelin synthase activity measurement. *Anal. Lett.*, **2012**, *45*(12), 1581-1589.
- [32] Yestrepesky, B.D.; Kretz, C.A.; Xu, Y.X.; Holmes, A.; Sun, H.M.; Ginsburg, D.; Larsen, S.D. Development of tag-free photoprobes for studies aimed at identifying the target of novel Group A Streptococcus antivirulence agents. *Bioorg. Med. Chem. Lett.*, **2014**, *24*(6), 1538-1544.
- [33] Seifert, T.; Malo, M.; Lengqvist, J.; Sihlbom, C.; Jarho, E.M.; Luthman, K. Identification of the binding site of chroman-4-one-based sirtuin 2-selective inhibitors using photoaffinity labeling in combination with tandem mass spectrometry. *J. Med. Chem.*, **2016**, *59*(23), 10794-10799.